Hyperanalytic Wavelet Packets

Ioana Firoiu[1,2], Dorina Isar[1]IEEE Member, Jean-Marc Boucher[2] IEEE Senior Member, Alexandru Isar[1]IEEE Member,
[1] Communications Dept., Electronics and Telecommunications Faculty, "Politehnica" University, Timişoara, Romania
ioana.firoiu@etc.upt.ro , dorina.isar@etc.upt.ro, alexandru.isar@etc.upt.ro
[2] Telecom Bretagne, Institut Telecom, UMR CNRS lab-STICC 3192, Brest, France
jm.boucher@telecom-bretagne.eu

***Abstract*—we introduce the hyperanalytic wavelet packets concept and we prove some of their properties: good frequency localization, quasi shift-invariance, quasi analyticity and quasi rotational invariance.**

I. INTRODUCTION

The Discrete Wavelet Transform (DWT) is commonly used in a wide range of signal and image processing applications. For the cases in which the frequency localization ensured by the DWT is not sufficient, the Discrete Wavelet Packets Transform (DWPT) [1] is used. Like the DWT, the DWPT is shift sensitive. In the two-dimensional case (2D), 2D-DWPT ensures a better directional selectivity than the 2D-DWT.

To reduce the shift-variance, several solutions based on the increase of the computation amount can be used. In [2] the Shift Invariant Wavelet Packets Transform (SIWPT) is proposed. When computing DWPT, down-sampling is achieved by ignoring all even-indexed or all odd-indexed terms. In contrast, when pursuing SIWPT, the down-sampling is carried out adaptively for the prescribed signal.

Another possible solution consists of the use of the Non-decimated Wavelet Packets Transform (NWPT), [3]. Through the use of delay blocks the odd samples (eliminated by down-sampling with 2 in the case of DWT or DWPT), are being recovered. The NWPT implementation scheme is equivalent to the DWPT implementation scheme, from which there were eliminated the down-samplers with 2. Because all the components left in the scheme are time-invariant linear systems (low-pass and high-pass filters), the NWPT is shift-invariant. Consequently, the NWPT is more redundant than the DWPT.

Apart from the great computation amount they imply, the two solutions of ensuring the translation-invariance in the one-dimensional case (1D) already discussed present also the disadvantage of reduced directional selectivity when generalized to the 2D case.

For this reason, the Complex Wavelet Packets Transforms (CWPT) [4, 5] were studied, Dual Tree Complex Wavelet Packet Transform (DTCWPT) [6], in particular. The latter is derived from the corresponding Dual Tree Complex Wavelet Transform (DTCWT) introduced by Kingsbury in [4].

One Complex Wavelet Transform (CWT) is based on Kingsbury's observation that approximate shift invariance can be obtained with a real biorthogonal transform by doubling the sampling rate at each scale. This is achieved by computing two parallel wavelet trees which are sub-sampled differently. The CWPT's disadvantage is the lack of analyticity, [6]. Analytic transforms have improved frequency localization.

This disadvantage is solved in [6], in which the DTCWPT is introduced, representing the generalization of the DTCWT, [7]. DTCWT consists of two trees, each implementing a DWT, the impulse responses of the filters used in the second tree being the approximate Hilbert transforms of the impulse responses of the filters used in the first tree. The coefficients are complex, having as real part the coefficients resulted from the first tree and for imaginary part those from the second tree. Consequently, the DTCWPT consists of two trees, each of them implementing a DWPT.

Using the definitions from [8] we have introduced in [9] the Analytic Wavelet Transform (AWT) and the Hyperanalytic Wavelet Transform (HWT) as alternatives to the DTCWT and 2D-DTCWT, offering an easier implementation and the possibility to use a larger number of mother wavelets.

In the present paper we propose the generalization of the AWT, and of the HWT, respectively, to the Analytic Wavelet Packets Transform (AWPT) and Hyperanalytic Wavelet Packets Transform (HWPT). In the next section we will present the 1D case, the AWPT. The 2D case, the HWPT, and the properties of shift invariance and directional selectivity, are discussed in section III. Section IV represents the conclusion of the present paper.

II. AWPT

The DWT is shift-sensitive and has a poor frequency localisation. The formula used for the computation of the DWT of a signal $f(t)$, using the mother wavelet $\psi(t)$ is:

$$DWT\{f(t)\} = \langle f(t), \psi(t) \rangle \tag{1}$$

To overcome the fisrt disadvantage we have introduced the AWT [9]. The analytical signal associated to the mother wavelets $\psi(t)$ can be written as:

$$\psi_a(t) = \psi(t) + i\mathcal{H}\{\psi(t)\} \tag{2}$$

Consequently, the AWT of a signal $f(t)$ is:

$$AWT\{f(t)\} = \langle f(t), \psi_a(t) \rangle \tag{3}$$

Taking into account relations (1) and (2), it can be written:

$$AWT\{f(t)\} = DWT\{f(t)\} + iDWT\{\mathcal{H}\{f(t)\}\} = \\ = \langle f_a(t), \psi(t)\rangle = DWT\{f_a(t)\}. \quad (4)$$

From equation (4) one can observe that the AWT's implementation uses two DWT trees: the first one is applied to the input signal and the second one to the Hilbert transform of the input signal. The resulted coefficients are complex, having for real part the output of the first tree and for imaginary part the output of the second tree. It was shown in [9] that the AWT is quasi shift-invariant.

In order to increase the frequency localization of the AWT, we can use the DWPT to replace the DWT in the AWT computation, leading to AWPT, a quasi shift-invariant well frequency-localized wavelet packets (WP) transform.

III. HWPT

The hyperanalytical mother wavelet associated to $\psi(x,y)$ is defined as:

$$\psi_h(x,y) = \psi(x,y) + i\mathcal{H}_x\{\psi(x,y)\} + j\,\mathcal{H}_y\{\psi(x,y)\} + \\ + k\mathcal{H}_y\{\mathcal{H}_x\{\psi(x,y)\}\} \quad (5)$$

where: $i^2=j^2=-k^2=-1$ and $ij=ji=k$, [8].

The HWT of an image $f(x,y)$ is:

$$HWT\{f(x,y)\} = \langle f(x,y), \psi_h(x,y)\rangle \quad (6)$$

Taking into account relation (5) it can be written:

$$HWT\{f(x,y)\} = \text{2D-DWT}\{f(x,y)\} + i\,\text{2D-DWT}\{\mathcal{H}_x\{f(x,y)\}\} + \\ + j\,\text{2D-DWT}\{\mathcal{H}_y\{f(x,y)\}\} + k\,\text{2D-DWT}\{\mathcal{H}_y\{\mathcal{H}_x\{f(x,y)\}\}\} = \\ = \langle f_h(x,y), \psi(x,y)\rangle = \text{2D-DWT}\{f_h(x,y)\} \quad (7)$$

So, the HWT of the image $f(x,y)$ can be computed with the aid of the 2D-DWT of its associated hyperanalytical image. The HWT implementation [9] uses four trees, each one implementing a 2D-DWT. The first tree is applied to the input image. The second and the third trees are applied to 1D discrete Hilbert transforms computed across the lines ($\mathcal{H}_x$) or columns ($\mathcal{H}_y$) of the input image. The fourth tree is applied to the result obtained after the computation of the two 1D discrete Hilbert transforms of the input image. HWT is both shift invariant and has an increased directional selectivity.

The HWT generalization proposed in the present paper is implemented in the scheme presented in fig.1. One can notice from this figure and from the equations above, that HWPT was obtained from HWT, by replacing the four trees computing the 2D-DWT with trees that compute the 2D-DWPT.

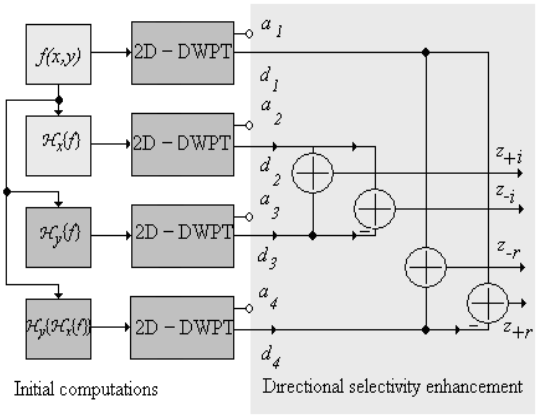

Figure 1. Proposed HWPT implementation.

There are several similarities between the proposed transforms and the complex wavelet packets transforms previously mentioned. As the CWPT and the DTCWPT, the HWPT uses four trees. Its quasi-analyticity comes from (6). The quasi shift-invariance is inherited from the HWT. The HWPT improves HWT's frequency localization in the same way the DWPT improves DWT's frequency localization. At last, HWPT has an increased directional selectivity, the same as the CWPT and the DTCWPT.

A. *Shiftability*

In the following, the HWPT's shift-invariance is exemplified. For this reason, the synthetic image in fig. 2 was created. On this image and on seven shifted versions of it, the 2D-DWPT and the HWPT, computed using the bior2.2 mother wavelets, are applied. For the computation of each of the five 2D-DWPTs necessaries to process each version of the image in fig. 2 (one for the computation of the 2D-DWPT and the other four for he computation of the HWPT), the same basis (the one obtained by the minimization of the entropy after the WP analysis of the image in fig. 2, marked in fig. 3) is used. In fig. 4 are represented the WP coefficients obtained after the application of the 2D-DWPT to the test image. For all five 2D-DWPTs, the same subband (also marked in fig. 3) is selected and all the WP coefficients corresponding to all the other subbands are cancelled. The subband marked in fig 3 is the only one considered in the case of the image in fig 2 and for all its seven shifted versions. The inverse transforms (corresponding to the 2D-DWPT and to the HWPT) are applied to the resulting coefficients. The results presented in fig. 4 correspond to the image from fig. 2.

For each of the eight input images, the energies of the corresponding response images are computed. The values obtained are presented in table I.

In order to obtain the degree of shift invariance, we calculate the mean m and the standard deviation sd of this energy sequence. Our degree of invariance is defined as:

$$\text{Deg} = 1 - sd/m \quad (8)$$

For the subband considered in the experiment described before there were obtained, using table I, the following values for the degree of shift-invariance: $Deg_{2D\text{-}DWPT}$ =0.3 and Deg_{HWPT} =0.81.

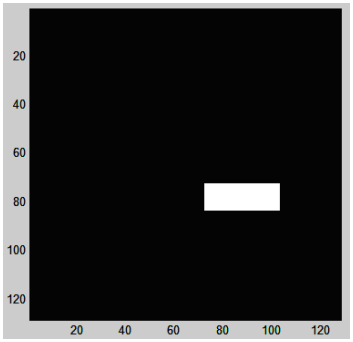

Figure 2. Synthetic image, conceived to study the shift-invariance of the HWPT.

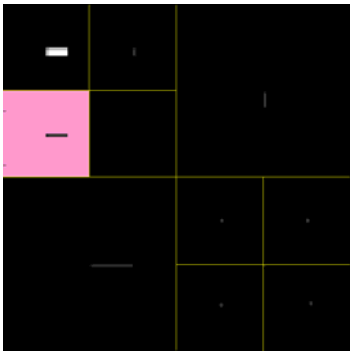

Figure 3. Image obtained after applying the 2D-DWPT on the image in the previous figure. The best basis is marked with yellow lines.

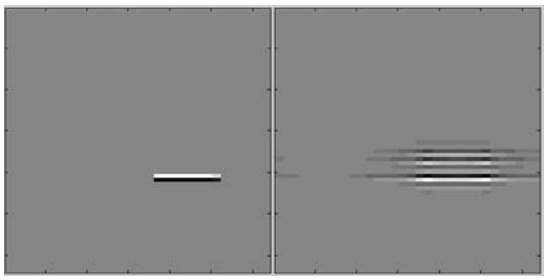

Figure 4. The response obtained using the 2D-DWPT (left) and the response obtained using the HWPT (right).

TABLE I. THE ENERGY SEQUENCES FOR THE 2D-DWPT AND HWPT.

	Best basis	EnergDWPT	EnergHWPT
1	3.6916	1.2390e+005	1.0469e+006
2	3.94033	5.9904e+005	1.5056e+006
3	3.94033	5.9904e+005	1.5056e+006
4	3.6916	1.2390e+005	1.0469e+006
5	3.6916	1.2390e+005	1.0469e+006
6	3.94033	5.9904e+005	1.5056e+006
7	3.94033	5.9904e+005	1.5056e+006
8	3.6916	1.2390e+005	1.0469e+006

B. Directional Selectivity

In the case of the 2D-DWT three directions are defined: horizontal, vertical and diagonal. The 2D-DWPT has an increased directional selectivity, compared to the 2D-DWT, as it can be concluded based on the comparative analysis of figures 5 and 6. In fig. 5 is presented the computation scheme for the 2D-DWPT (with two iterations) (center) and the spectrum of the input image (left). Supposing that the low-pass filter, *h* and the high-pass filter, *g*, are ideal, at the outputs 2 – 8 are obtained the images with the spectra represented at right.

The scheme implements the 2D-DWT with two iterations, if the outputs: 1–4, 18, 19 and 20 are selected. In the case of the 2D-DWPT there can be selected other outputs too, according to the criterion the best basis is chosen on. For example, the outputs 1–16 can be selected.

The images from the first seven outputs of fig. 5 (2–8), contain six different directions: ±arctg(2), ±arctg(1/2), ±arctg(1), ±arctg(1/3), ±arctg(2/3) and ±arctg(1/4). Consequently, the 2D-DWPT's directional selectivity is better than that of the 2D-DWT.

As shown in [9], HWT has six preferential directions. It is able to separate the pairs of directions selected by the 2D-DWT. For the input image with the spectrum in fig. 5, the spectra of the 16 outputs of the HWPT corresponding to the first 4 outputs of the 2D-DWPT from fig. 5 are presented in fig. 6. HWPT's directional selectivity is sufficiently high to consider it quasi rotational invariant.

In the following, the theoretical properties of the HWPT regarding its directional selectivity, already presented, are illustrated using an example. At first, the synthetic image presented in fig. 7, contains 8 preferential directions: 0°, arctg(1/2)°, 45°, arctg(2)°, 90°, -45°, -arctg(1/2)° and -arctg(2)°. It can be noticed that these are perpendicular in pairs of two (0° and 90°, 45° and -45°, arctg(2)° and -arctg(1/2)°, respectively arctg(1/2)° and -arctg(2)°).

We have applied to this image the 2D-DWPT with two iterations, using Daubechies 20 mother wavelets and we have obtained the coefficients and the best basis (from the entropy minimization point of view), represented in the left image of fig. 8. Next we have computed its HWPT using the best basis obtained before for the computation of all the four 2D-DWPT components. The $\mathrm{Im}\{z_+\}$ coefficients obtained are represented in the right image from fig. 8. Analyzing the left image in fig. 8 one can notice the validity of the 2D-DWPT directional selectivity analysis, presented in fig. 5. For example, it can be seen that at output 8 are selected the directions $\pm\mathrm{arctg}(1/2)$ °. It is also observed the 2D-DWPT's incapacity to differentiate perpendicular directions (at output 9, for instance, we can observe directions arctg(2)° and –arctg(1/2)°) . Comparing the images in the left and in the right of fig. 8, it is observed that HWPT has a directional selectivity superior to that of 2D-DWPT. For example, at output 4 of the left side image directions ±arctg(1) are observed, while at output 4+ (same output of the right side image) there is only direction arctg(1).

Finally, in fig. 9 is presented a comparison between 2 sets of coefficients of the HWPT: $\mathrm{Im}\{z_+\}$ and $\mathrm{Im}\{z_-\}$.

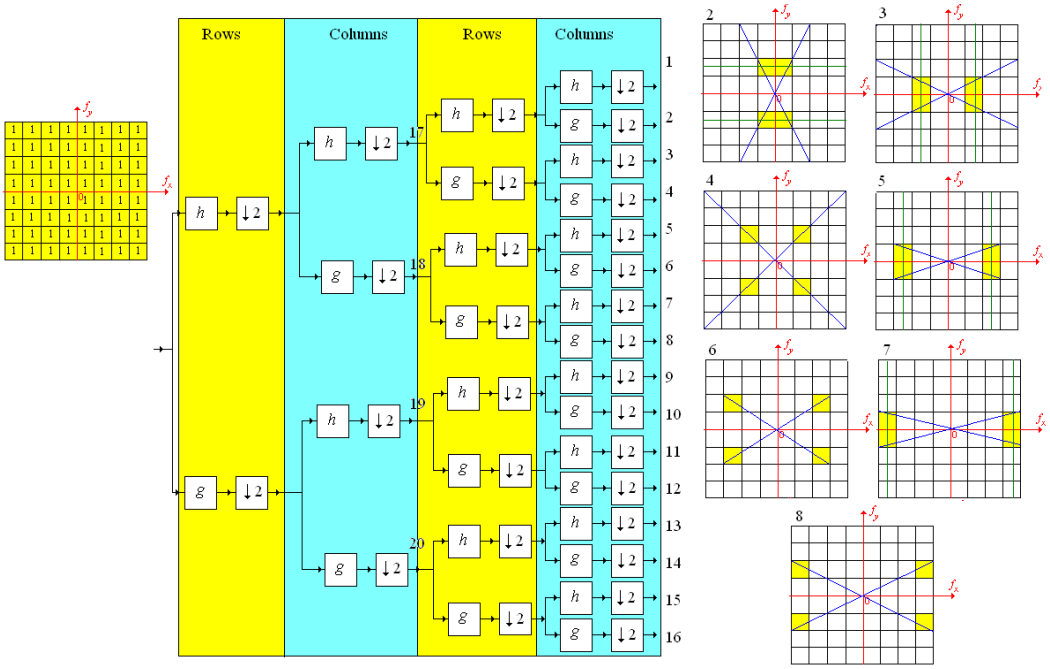

Figure 5. 2D-DWPT with two iterations. The low-pass filter *h* and the high-pass filter *g* are considered ideal. The images from the first seven detail outputs are marked.

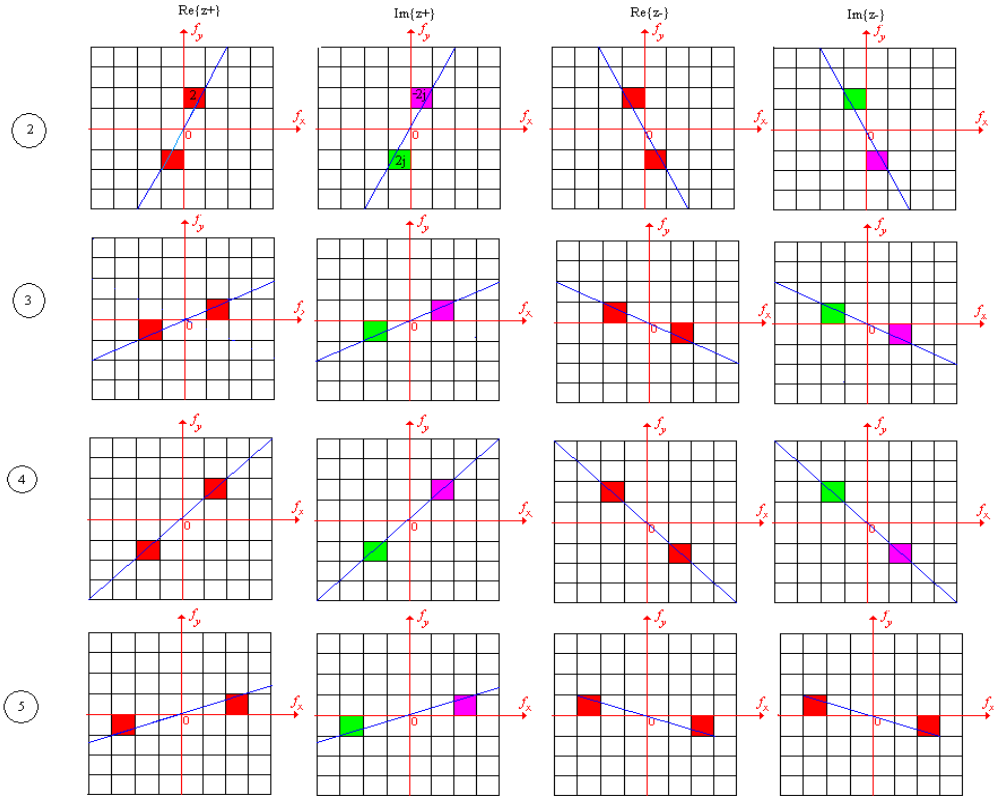

Figure 6. HWPT can separate the directions of angles arctg(1/2), arctg(1), arctg(1/3), arctg(2) from the directions of angles -arctg(1/2), -arctg(1), -arctg(1/3), -arctg(2).

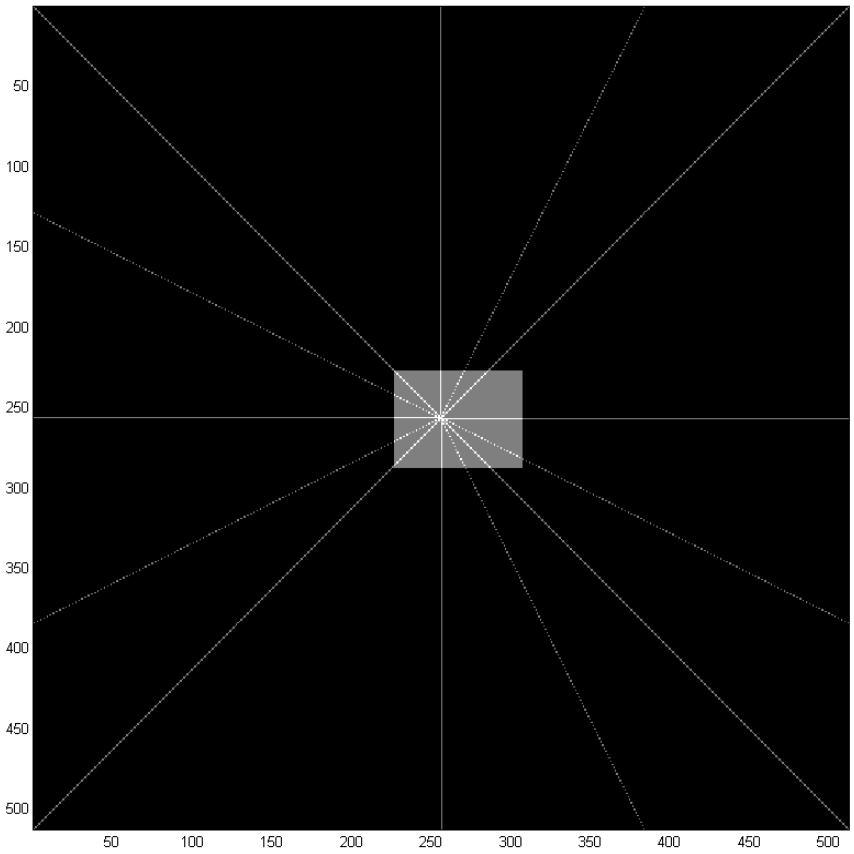

Figure 7. The input image contains some prefferential directions.

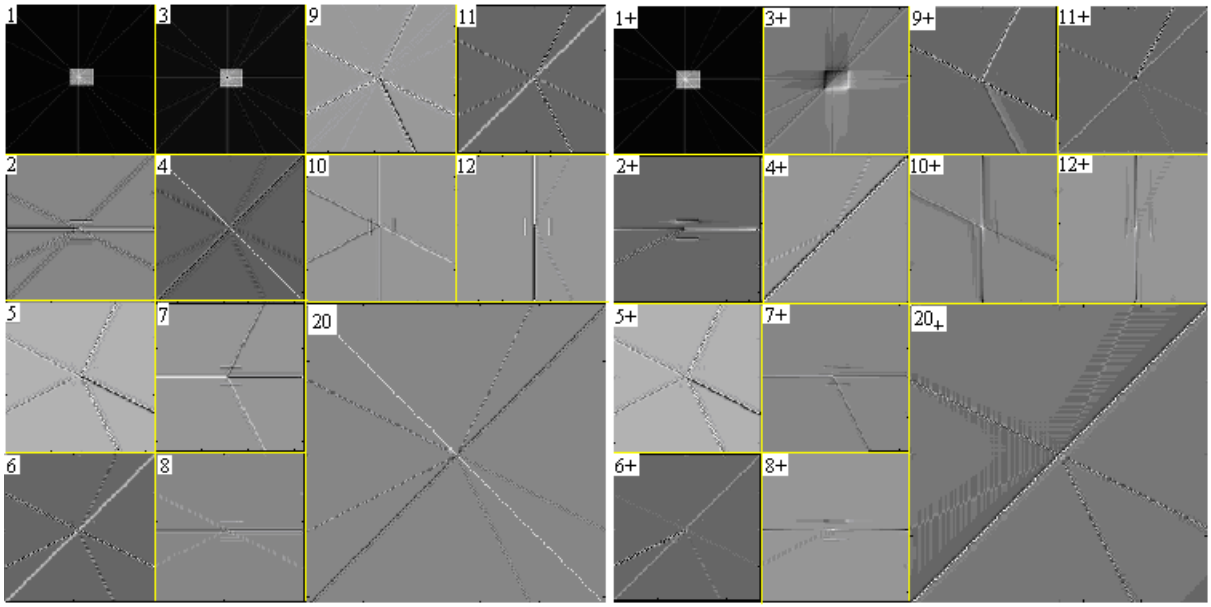

Figure 8. Comparison between the 2D DWPT (left) and HWPT (the coefficients $\mathrm{Im}\{z_+\}$, more precisely) (right) of the image in fig. 7. The subbands were indexed according to fig. 5 and 6.

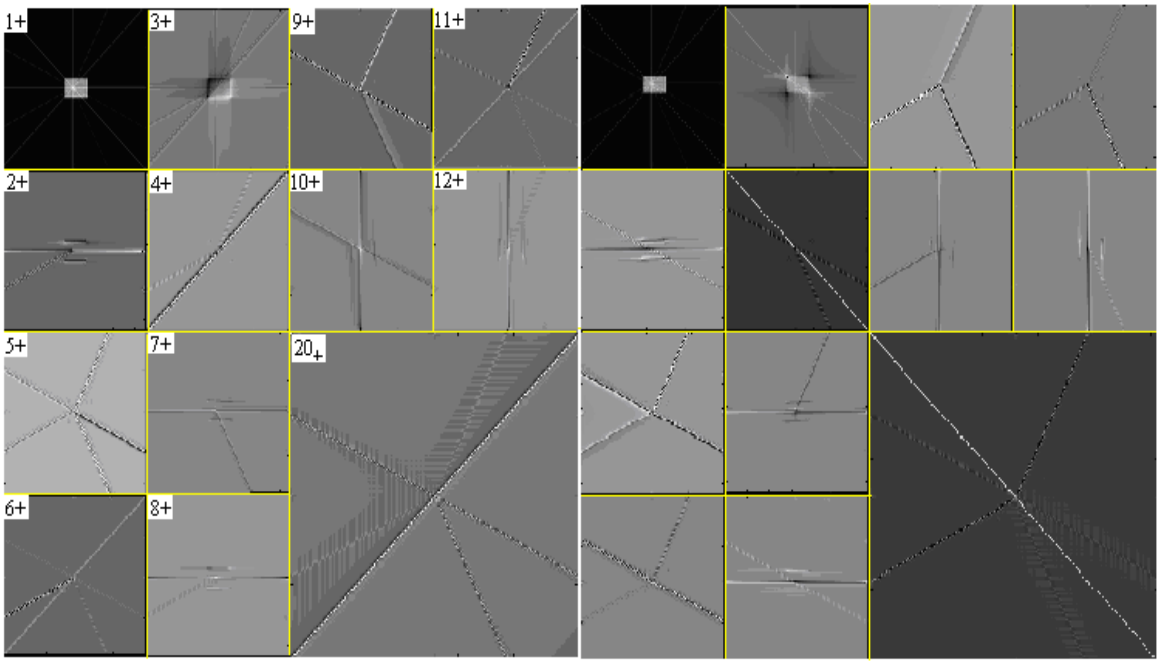

Figure 9. A comparison of two sets of outputs of the HWPT. The outputs corresponding to the coefficients $\mathrm{Im}\{z_+\}$ are represented in the left picture. The same outputs corresponding to the coefficients $\mathrm{Im}\{z_-\}$ are represented in the right picture. The left picture contains preponderently positive angle directions while the right picture contains mostly negative angle directions.

The good directional selectivity of the HWPT can be observed analyzing fig. 9. The images in the left picture contain mostly positive directions (see for example the output 4_+). The corresponding outputs in the right picture contain with preponderance negative directions (the directions contained at the output 4_- are of negative angles and are orthogonal on the directions that can be found at the output 4_+).

IV. Conclusion

In this paper are proposed the hyperanalytic wavelet packets and are presented some of their properties:

- good frequency localization,
- quasi shift-invariance,
- quasi analyticity,
- quasi rotational invariance.

The results of the experiments presented prove that HWPT is a viable alternative for the 2D-CWPT and, respectively, the 2D-DTCWPT. HWPT's advantage compared to 2D-CWPT and, respectively, the 2D-DTCWPT, is given by its increased flexibility in choosing the mother wavelets, because it can be implemented using any of the functions of this type introduced with the orthogonal or bi-orthogonal wavelet transforms.

Considering HWPT's very good frequency localization, we intend to use this transform in the future for texture image processing. We have in mind image denoising applications. It is already known that using different mother wavelets different denoising quality is obtained. The mother wavelets selection procedure is difficult because the images are very complicated signals. A possible selection criterion is based on the time-frequency localization. But different regions of an image have different time or frequency localizations. For example the textured regions have better frequency localization than the homogeneous regions. This is why we intent in the future to denoise the textured regions with WP. We intent to use the HWPT to take advantage of its useful properties: quasi shift-invariance, quasi analyticity and quasi rotational invariance.

V. References

[1] M.V.Wickerhauser, "Adapted Wavelet Analysis from Theory to Software", *AK Peters,* Ltd., 1994.

[2] I. Cohen, S. Raz and D. Malah, "Orthonormal shift-invariant wavelet packet decomposition and representation", *Signal Processing*, 57(3):251-270, January 1997.

[3] Pesquet, J.C., Krim, H., Carfantan, H. (1996), "Time-invariant orthonormal wavelet representations", *IEEE Trans. Sig. Proc.,* 44, 1964-1970.

[4] N. Kingsbury, "The dual-tree complex wavelet transform: a new efficient tool for image restoration and enhancement", *Proc. of EUSIPCO*, pp. 319 – 322, (Rhodes, Greece), 1998.

[5] André Jalobeanu, Laure Blanc-Feraud and Josiane Zerubia, "Natural image modeling using complex wavelets", in *Wavelets X, SPIE Symposium*, San Diego, CA, Aug. 2003.

[6] Ilker Bayram and Ivan W. Selesnick, "On the Dual-Tree Complex Wavelet Packet and M-Band Transforms", *IEEE Trans. Signal Processing*, 56(6) : 2298-2310, June 2008.

[7] N.G.Kingsbury, "Complex wavelets for shift-invariant analysis and filtering of signals", *J. of Appl. And Comp. Harm. Analysis*, 10(3):234-253, May 2001.

[8] C. Davenport, "Commutative Hypercomplex Mathematics", http://home.comcast.net/~cmdaven/nhyprcpx.htm

[9] I. Adam, C. Naforniță, J-M. Boucher and A. Isar, "A Bayesian Approach of Hyperanalytic Wavelet Transform Based Denoising", *Proc. IEEE Int. Conf. WISP'07*, Alcala de Henares, Spain, October '07, 237-24.